Advanced Composites and Hybrid Materials (2024) 7:129
https://doi.org/10.1007/s42114-024-00940-4

RESEARCH

Formaldehyde-free high-strength low-density wood biocomposites via corrugation and self-bonding of wooden cell

Yan Yang[1,2] · Xiaochen Yue[1] · Cheng Li[1] · Zeinhom M. El-Bahy[3] · Saad Melhi[4] · Hamdy Khamees Thabet[5] · Xiaoyi Duan[1] · Nyuk Ling Ma[6,7] · Yafeng Yang[1] · Su Shiung Lam[2,8] · Wanxi Peng[1]

Received: 18 March 2024 / Revised: 15 July 2024 / Accepted: 18 July 2024 / Published online: 29 July 2024

Abstract

In alignment with global sustainable development strategies and the growing demand for green manufacturing practices in engineered wood production, an innovative method has been developed for incorporating hot pressing techniques, minimal energy consumption, and the complete elimination of adhesives. This approach achieved a 100% conversion of waste palm wood into sustainable natural biocomposites suitable for use in structures and furniture. Analysis shows that the biocomposites forms strong internal bonding through mechanical "nail like" nanomaterials, ester bonds, and ether bonds. Unlike conventional furniture materials, which rely on hazardous formaldehyde-based adhesives, this biocomposites boasts an internal bonding strength of 1.652 MPa—four times higher than typical materials. Additionally, it is lightweight, with a density of less than 1 g/cm^3, offers excellent friction resistance, and is dense with only 0.67% internal porosity. The composite materials eliminate the use of toxic adhesives, addressing concerns regarding potential harmful emissions from formaldehyde-based VOCs and ensuring higher indoor air quality. This surpasses the performance of existing structures and furniture materials that rely on synthetic adhesives. The method achieves a 100% conversion of waste palm wood into biocomposites, offering a cost-effective and profitable alternative. This provides a novel solution for developing new structural and furniture materials.

Keywords Palm biomass · Biocomposites · Lightweight · Nano-scratch · Micro-CT

1 Introduction

Wood as one of the four major building materials in the world (including cement, masonry, and steel) [1, 2], is an extremely complex biocomposites [3]. Wood has inherent characteristics that differ from other materials: biological characteristics, porous properties, anisotropy and variability, durability, regeneration, and modifiability [4–8]. Although wood has made significant contributions to national economic and city construction, single wood products or wood materials (including various Engineered wood) can no longer meet the needs of human social development. Conventional biocomposites are limited by mechanical processing conditions, and the strength of wood cannot meet the requirements of many engineering structures [9].

Wood composites using formaldehyde-based adhesives have improved in this respect [10, 11], but the long-term release of formaldehyde in wood will cause disease and harm to human health, and increase the risk of indoor environmental pollution [12]. This is due to the fact that chemically synthesized adhesives, exemplified by urea–formaldehyde and phenol–formaldehyde, frequently harbor volatile organic compounds (VOCs), which, upon release, emit formaldehyde into the ambient surroundings [13, 14]. Formaldehyde and VOCs are detrimental, posing the potential to induce adverse health effects, such as irritation, headaches, and nausea. Prolonged exposure to these substances may result in severe consequences for humans, encompassing the development of liver disease and cancer [15, 16]. In order to solve the fundamental problem of formaldehyde release and weather resistance in wooden cells, since Cai Lun improved folk papermaking methods in 105 AD, the dream of wood scientists for 2000 years has been to achieve high-strength self-binding of wooden cells. However, the existing adhesive free bonding technology has problems and bottlenecks such as low

Yan Yang, Xiaochen Yue and Cheng Li these authors equally contributed to this work as co-first authors.

Extended author information available on the last page of the article

bonding strength, cumbersome processes, low efficiency, and unclear self-bonding mechanism, which restrict the development of low-cost and efficient green composite processing technology for wood fibers.

The hot pressing method is a commonly employed processing technology for manufacturing composite materials [17, 18]. Within this method, raw materials typically manifest in either flake or granule form, undergoing direct compression into the desired shape amidst conditions of elevated temperature and pressure [19]. Conventional methods typically entail the mixing of raw materials with adhesives, followed by pressing, extrusion, and molding (including injection molding and compression) [20]. Moreover, they necessitate the setup of additional auxiliary equipment, such as specialized heating, exhaust, drying, and cooling systems, which prolongs the duration required for completing the curing and bonding processes of materials [21]. The hot pressing method involves the direct application of high temperature and pressure to compress the raw materials, facilitating the bonding of material molecules to create a robust composite structure. Additionally, processing temperatures and pressures in conventional methods may fluctuate depending on the characteristics of the material and binder, frequently necessitating individual adjustments for each material [21]. However, in the hot pressing method, the processing temperature and pressure remain generally stable and controllable, as they are regulated through the parameter settings of the hot press and remain unaffected by the type of raw material used. In general, compared with conventional methods, the hot pressing method has the advantages of simple process principle, stable processing temperature and pressure, and fast molding speed.

At the same time, alongside the swift progression of technology, elevated demands have been articulated for the wood science community [22–24]. Palm wood is a common tree that originated in China and is currently distributed around the world. Palm trees have high economic value, and Indonesia and Malaysia are one of the few palms' oil producing and exporting countries in the world, with palm cultivation areas reaching 14.8 million hm^2 and 5.4 million hm^2, respectively [25–27]. To ensure palm oil production, 25-year-old palm trees need to be harvested and renewed [28]. Most of the fallen palm trees are placed in plantations or burned, seriously polluting the environment and causing a large amount of resource waste. The sustainable use of palm trees is an important way to protect the environment and promote economic development. In Malaysia, workers spin and cut some harvested palm trees into veneer for the production of plywood [29, 30]. Due to the lower density of the inner layer of palm trees compared to the outer layer, and their soft tissue, improving the quality and compressive strength of plywood has become a major technical challenge.

Therefore, a series of experiments were conducted to explore the conversion of palm wood, a raw material, into biocomposites. Subsequently, a low-energy one-step production process using hot pressing as a potential technique. In contrast to conventional furniture materials dependent on formaldehyde-based adhesives, this biocomposites eschews toxic adhesives, thereby circumventing the issue of deleterious formaldehyde emissions. Concurrently, it transcends the conventional theoretical framework of adhesive-free wood bonding, thus achieving an original theoretical innovation in formaldehyde-free wood composite materials and offering a novel approach to advancing the development of new structural and furniture materials.

2 Materials and methods

2.1 Preparation of biocomposites

The palm wood obtained from Terengganu University in Malaysia was dried and crushed into powder (particle size: 0.25–0.425 mm) to imitate the wood waste generated by the furniture industry. Before conversion, all waste underwent a 12-h drying phase at 55 °C, followed by storage at 5 °C. Palm sawdust was pressed using a hot press at 147 MPa [31] for 10 to 35 min to produce biocomposites (size: 50 mm long × 50 mm wide × 7 mm thick). Biocomposites with varied mechanical properties (Fig. 1 and Table S1) were acquired through the manipulation of temperature, pressure, and pressing duration, denoted as Y1, Y2, Y3, Y4, Y5, Y6, Y7, Y8, Y9, and Y10, respectively. Through using various physical and chemical analysis methods, three tests were conducted on each biocomposites sample to determine and describe the reactivity, chemical transformation, and structural evolution of wood fiber biocomposites, thereby revealing their self-adhesion mechanism.

2.2 Internal bonding strength (IBS) and compressive strength

According to the Chinese national standard *GB/T 17657–2013*, the IBS (internal bonding strength) of the samples was determined [31]. The IBS was measured by subjecting the 50 mm × 50 mm × 7 mm sample to tension until failure. The IBS was computed by dividing the maximum failure tension by the vertical surface area. The sample underwent testing, positioned on a chuck and affixed with epoxy resin, enabling the measurement and assessment of the bonding quality between fibers within the sample. Low IBS values may lead to sample stratification, while a higher

IBS indicates better resistance to temperature variations and a reduced risk of cracking [32, 33].

The compressive strength of the samples was measured using a cement flexural and compressive constant stress testing machine (Model HYE-300B). The load was applied uniformly at a rate of 1.1 kN/s ± 100 N/s on the side surface of a half-prism until failure occurred. The compressive strength Rc (MPa) of the sample was calculated according to Eq. (1). Extended Data Table S2 shows the compressive strength test results of the samples.

$$Rc = \frac{Fc}{A} \quad (1)$$

where: Fc — the maximum load at failure (kN), A — the area of the compressed section (m^2).

2.3 FTIR and thermogravimetric analyses

Extraction of samples was performed utilizing KBr discs incorporating 1.00% finely ground specimens. The FT-IR spectra for each sample were acquired employing a Thermo Fisher Scientific iS10 spectrophotometer, with a spectral range of 500–4000 cm^{-1}.

The powder of the sample was also analyzed by thermogravimetric analyzer (TGA-Q500, TA Instruments) to investigate the material content (such as water, volatile matter), thermal stability, reaction kinetics and decomposition stage of the sample [31]. The nitrogen release rate is 60 mL/min. The TG temperature program starts at 30 °C and increases at a heating rate of 25 °C/min to 750 °C.

2.4 Nanoindentation and nanoscratch analyses

The samples were tested using the TI-980 nanoindentation instrument (Bruker, United States). The sensor used a 10-mN range two-dimensional mechanical sensor, with a maximum loading force of 8 mN and a loading time of 5 s. The load was maintained for 2 s and unloaded for 5 s. The testing method for the sample is 3 × 4 arrays, testing 12 points per sample, with a spacing of 100 μm [34].

Use a 3D scratch tester (Rtec, China) to perform scratch testing on the sample. In the 3D scratch test, a tip scratch head with a radius of 0.1 μm was used, with a loading force of 10 N, a running speed of 0.08 mm/s, and a scratch length of 3 mm [35]. A 20 × confocal lens was used to image the scratch morphology.

2.5 Additional analyses

The anti-wear characteristics of the sample were tested using a friction tester (Rtec, China) [36, 37]. The testing instrument uses a grinding ball with a radius of 9.3 mm, a loading force of 5 N, a friction frequency of 1 HZ, a friction stroke of 10 mm, and a friction time of 10 min. A 20 × confocal lens is used to image the morphology of the sample after friction.

Using XRadia Context 3D Micro CT (ZEISS, Germany) to scan and image the samples, observe the internal microstructure of the biocomposites. The sample was scanned and imaged using a voxel resolution of 22.0 μm, with a field of view range of Ö 66.0 * 44.0 mm, a scanning energy of 60 kV, a scanning power of 5 W, and a scanning time of 0.5–1 h. Use a 3.0-μm voxel resolution to perform high-resolution, high contrast scanning imaging of the local area of the sample. The field of view range is Ö 9.0 * 6.0 mm, with a scanning energy of 60 kV, a scanning power of 5 W, and a scanning time of 0.8 h.

The surface morphology of the biocomposites was analyzed using an S-3400N scanning electron microscope (SEM) (Hitachi Ltd., Japan).

Formaldehyde emission of biocomposites was measured in accordance with the Chinese national standard "Test methods of evaluating the properties of wood-based panels and surface decorated wood-based panels" (*GB/T 17657–1999*).

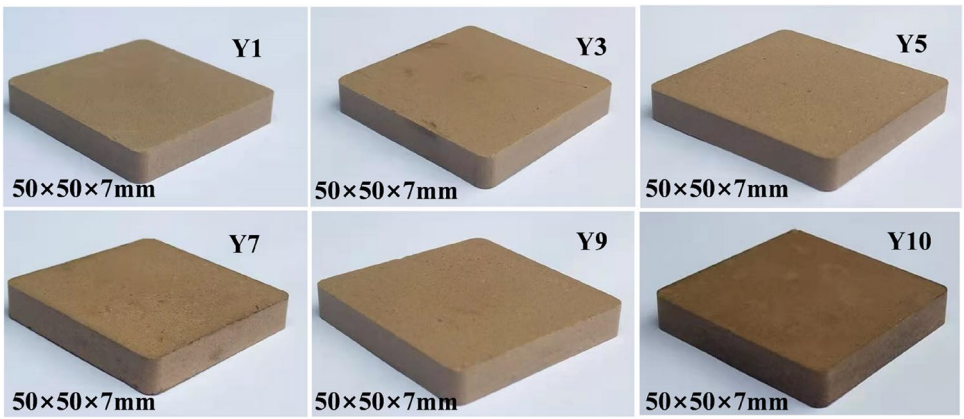

Fig. 1 Palm biocomposites (size: 50 mm long × 50 mm wide × 7 mm thick)

2.6 Statistical analyses

Graph Pad Prism9.0 software was used for the graphical presentations, while a paired Student's *t*-test was used to test for group references (significant level set to $p < 0.05$).

3 Results and discussion

3.1 Physical and chemical analyses

The sample biocomposites was tested using FT-IR and Fig. 2a shows several clear spectral peaks. The absorption peaks of each spectrogram reflect the types of functional groups contained in the substance and its chemical environment [38, 39]. In the 3390 cm^{-1} band, the O–H bond tensile vibration of aromatic and Aliphatic compound is mainly formed, and in the 1030 cm^{-1} band, the C-O bond tensile vibration of aldehydes, esters and carbohydrates is mainly formed. The peak absorption at 1610 cm^{-1} is caused by the stretching vibration of the carbon–carbon double bond (C = C) in alkanes. The peak absorption at 1740 cm^{-1} is attributed to the stretching vibration of the carbonyl group (C = O) present in aldehydes, ketones, acids, and esters. The ability to improve fiber self-adhesion is further evidenced by the strength of absorption peaks observed at the FT-IR transmission peak, encompassing various functional groups including O–H bonds, aldehydes, carbohydrates, ketones, alkanes, and ester C = O bonds [40]. Through Chemical bonds, including hydrogen bonds, ester bonds, and ether bonds, more robust chemical connections are established between compounds in biocomposites [31].

In a high-purity nitrogen atmosphere, palm wood undergoes a series of processes, including oxidation, dehydration, condensation, reduction, and decomposition, ultimately leading to weight loss [41]. The thermal weight loss curves for various biocomposites are depicted in Fig. 2b and Fig. S1. During the process of heating to 750 °C at room temperature, the thermal weight loss curve of the sample biocomposites is divided into three stages. In the first stage of weight loss at 30–235 °C, the total weight loss rate of the sample biocomposites is around 2%, mainly due to the evaporation of some water vapor and low boiling point small molecules. When the temperature rises to 250 °C, the weight of the sample begins to sharply decrease, and the thermal weight loss rate reaches its maximum at 347 °C. This stage is mainly due to the cleavage of the heavy components (such as sugars, phenols, esters, and carbohydrates) in the biocomposites. At 500 °C, the weight loss rate of the sample reaches about 28%. With the ongoing increase in temperature, the weight of the sample biocomposites exhibited only a marginal decrease. When the final temperature reached 750 °C, the weight of various sample biocomposites remained at 21–27%, among which the Y10 sample biocomposites with paraffin added had the most weight loss, and the final weight loss rate reached 79%.

Similarly, SEM analysis shows that the fiber structure is tightly bound in the hinge network (Fig. 2c). In addition, all broken and fragmented cell wall fibers will cause the intertwined fragments between the fibers to completely close (Fig. 2c and d). In summary, this creates a biocomposites with an intricate interface structure formed by interlacing networks of fibers. Micro CT analysis (Fig. 2d) confirmed that the Tight junction fiber network formed a dense interface structure in the biocomposites [42]. Figure 2c shows the fragmentation of cells, which generates various subminiature substances, enhances physical and chemical interconnections, thereby improving densification.

3.2 Strength and hardness

Internal Bond Strength (IBS) tests were conducted on each palm biocomposite, and the corresponding test results are illustrated in Fig. 3b. According to the results of Y1, Y2, Y3, and Y4, when the insulation time is 25 min, the IBS value of palm biocomposites obtained at 170 °C is the highest, reaching 1.308 MPa (Fig. 3c). During the process of 150–170 °C, as the temperature continues to rise, the IBS value gradually increases. Comparing the results of Y3, Y5, Y6, Y7, Y8, and Y9 samples, it was found that under the same temperature (170 °C) conditions, the IBS value of palm biocomposites obtained at a holding time of 25 min was the highest 1.308 MPa (Fig. 3d). The IBS value of palm Y10 with the addition of paraffin increased compared to the corresponding value of the control group, reach 1.652 MPa. The internal bond strength of palm biocomposites is also superior to that of fiber biocomposites reported by Shi et al. (1.52 MPa) [43]. The addition of paraffin made the wood fibers tightly bonded, enhanced their surface hardness and internal bonding strength, and made them more wear-resistant and wear-resistant. This process condition provides reference and reference for the production and processing of palm biocomposites.

Based on the aforementioned considerations, it is deduced that the selection of an appropriate hot-pressing temperature (170 °C) and holding time (25 min) is pivotal in the fabrication of palm biocomposites. Utilizing hot-pressing technology proves effective in enhancing the interface compatibility between the matrix and filler, facilitating uniform filler dispersion, and elevating the overall performance of the composite material. In comparison with both Chinese National Standards and American National Standards for Medium Density Fiberboard (MDF) and Particleboard (PB) in China,

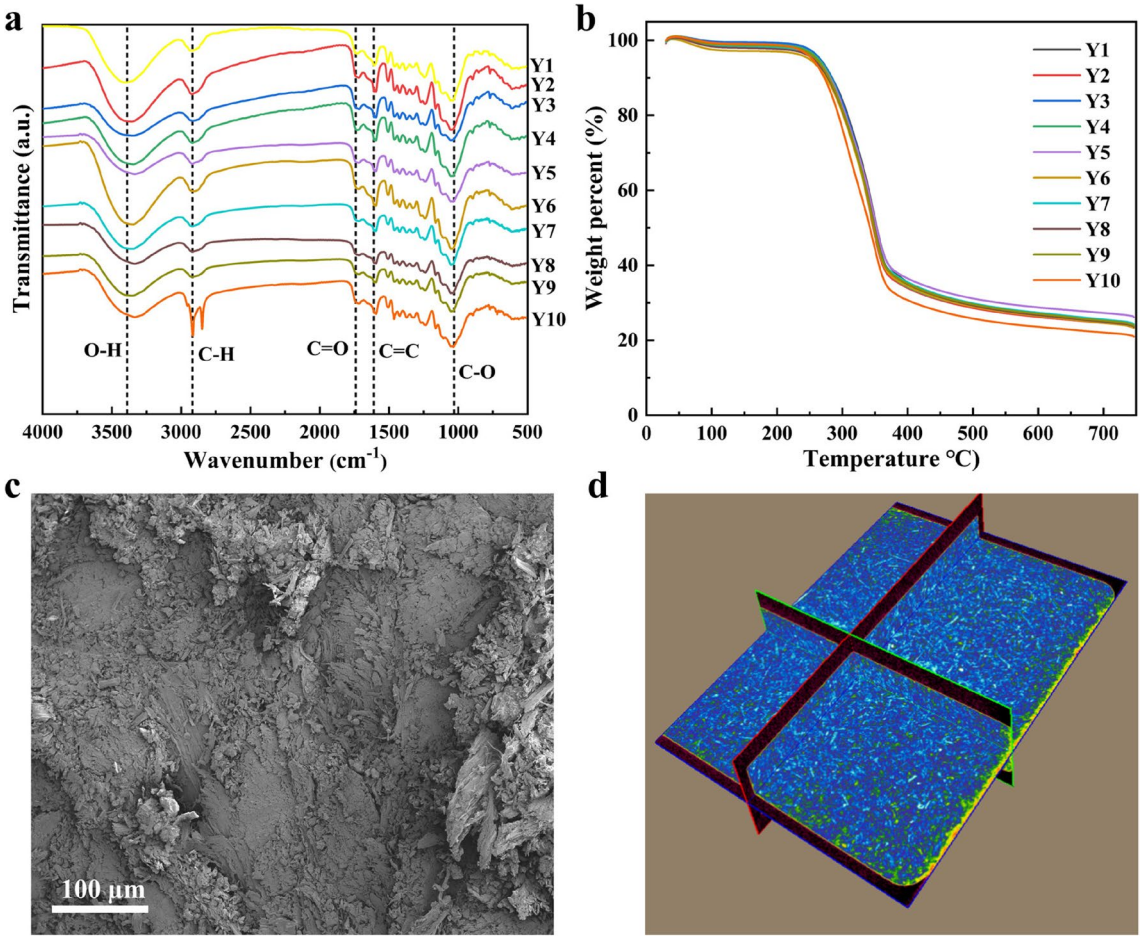

Fig. 2 **a** FTIR Spectrogram of palm biocomposites. **b** Thermal weight loss curve of palm biocomposites. **c** SEM micrographs of palm biocomposites (Y10). **d** The micro-CT (voxel resolution of 22 μm) of palm biocomposites (Y1)

this biological composite demonstrates significantly elevated adhesive strength, ranging between 0.648 and 1.652 MPa. This range is 2 to 4 times greater than the specified values for commercial MDF (U.S., ≥ 0.8 MPa; CN, ≥ 0.6 MPa) and PB (U.S., ≥ 0.6 MPa; CN, ≥ 0.4 MPa) outlined in the national standards [31]. The creation of shorter and finer wood particles led to improved packing efficiency, allowing for greater IB strength. The smaller size of the particles enabled them to fit together more snugly, much like the way puzzle pieces fit together to create a completed picture. This intimate contact between the particles translated into increased IB strength, as the pieces of wood were held together more securely, reminiscent of the way bricks in a wall are tightly mortared to provide support and stability.

In addition, compressive strength tests on palm biocomposites and found that the compressive strength values of Y1, Y2, Y3, and Y4 biocomposites were all greater than 90 MPa, with a compression rate of 11–15% (Table S2). The specific strength value (strength/density) of Y1 biocomposites is the highest, at 177.88 MPa·cm^3/g (Table S3), and similar to aluminum alloy materials (244 MPa·cm^3/g) [44] commonly used in industry. The maximum compressive strength value of palm biocomposites (139.638 MPa) is 2 times the compressive strength specified for bridge bearings (70 MPa) as seen in Fig. 3a [45]. This groundbreaking development means that biocomposites have become an important breakthrough in replacing concrete and pine in structural applications such as architecture and furniture (Fig. 3g). This breakthrough technology not only breaks the limitations of traditional wood, but also provides strong support for sustainable development in the future.

Nanoindentation testing was conducted to evaluate the micro and nanomechanical properties of biocomposites. The exquisite nanoindentation technique carries the distinction of high resolution and depth sensing abilities, establishing it as a formidable toolbox for gauging the nanomechanical attributes of minute materials. This paves a path towards exploring the mechanical behavior of materials at the nanoscale, deciphering the complex interactions that occur between materials and their environment

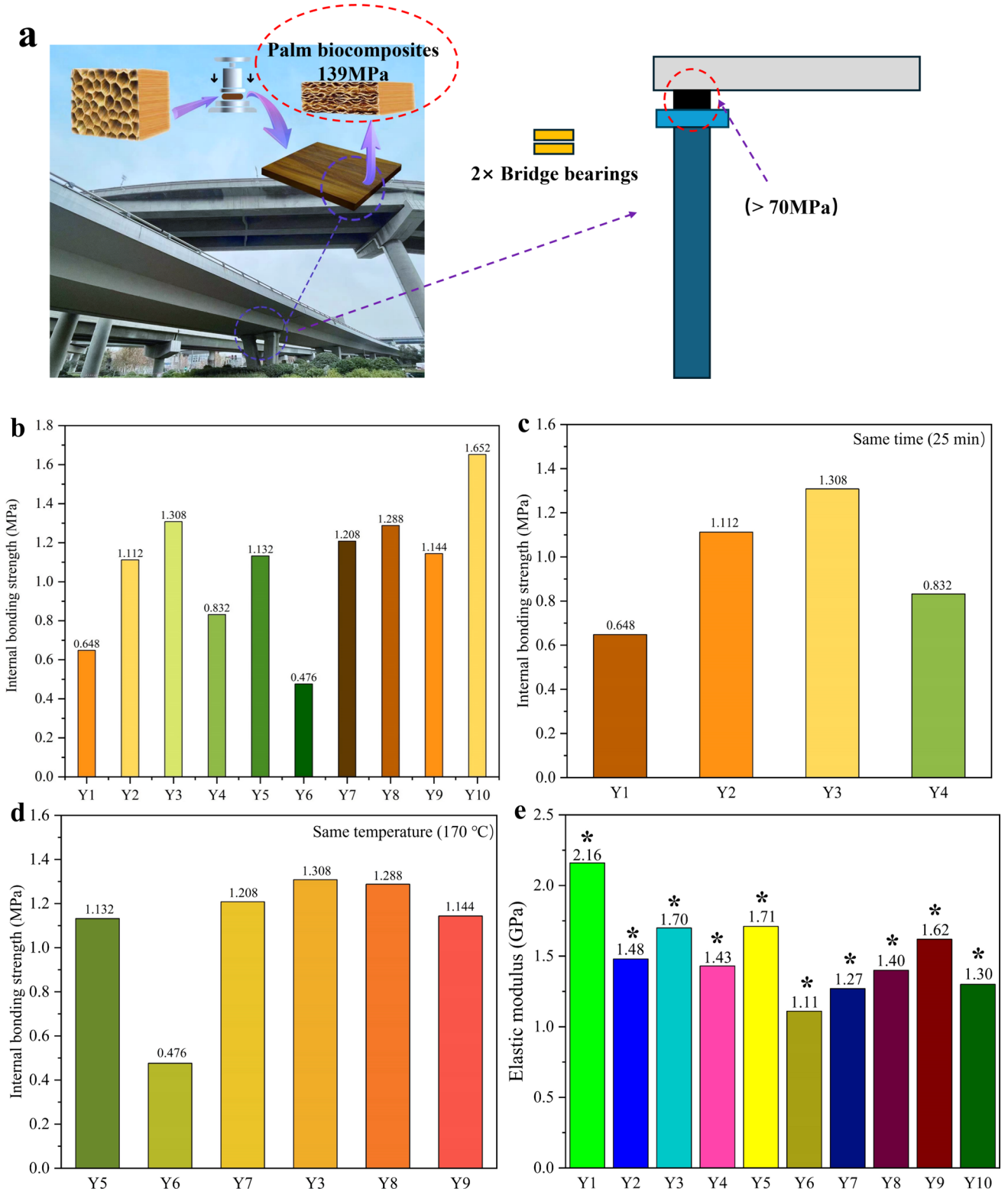

Fig. 3 **a** Compressive strength of bridge bearings and palm biocomposites. **b** Internal bonding strength of palm biocomposites. **c** Internal bonding strength of palm biocomposites obtained under the same insulation time. **d** Internal bonding strength of palm biocomposites obtained under the same temperature. **e** Elastic Modulus of palm biocomposites. **f** Hardness of palm biocomposites. **g** The compressive strength of various common building materials. **h** Surface morphology images of palm biocomposites (Y10) after nanoindentation. **i** Surface morphology images of palm biocomposites (Y10) after nanoindentation, obtained using a profilometer. "*" Significance value < 0.05

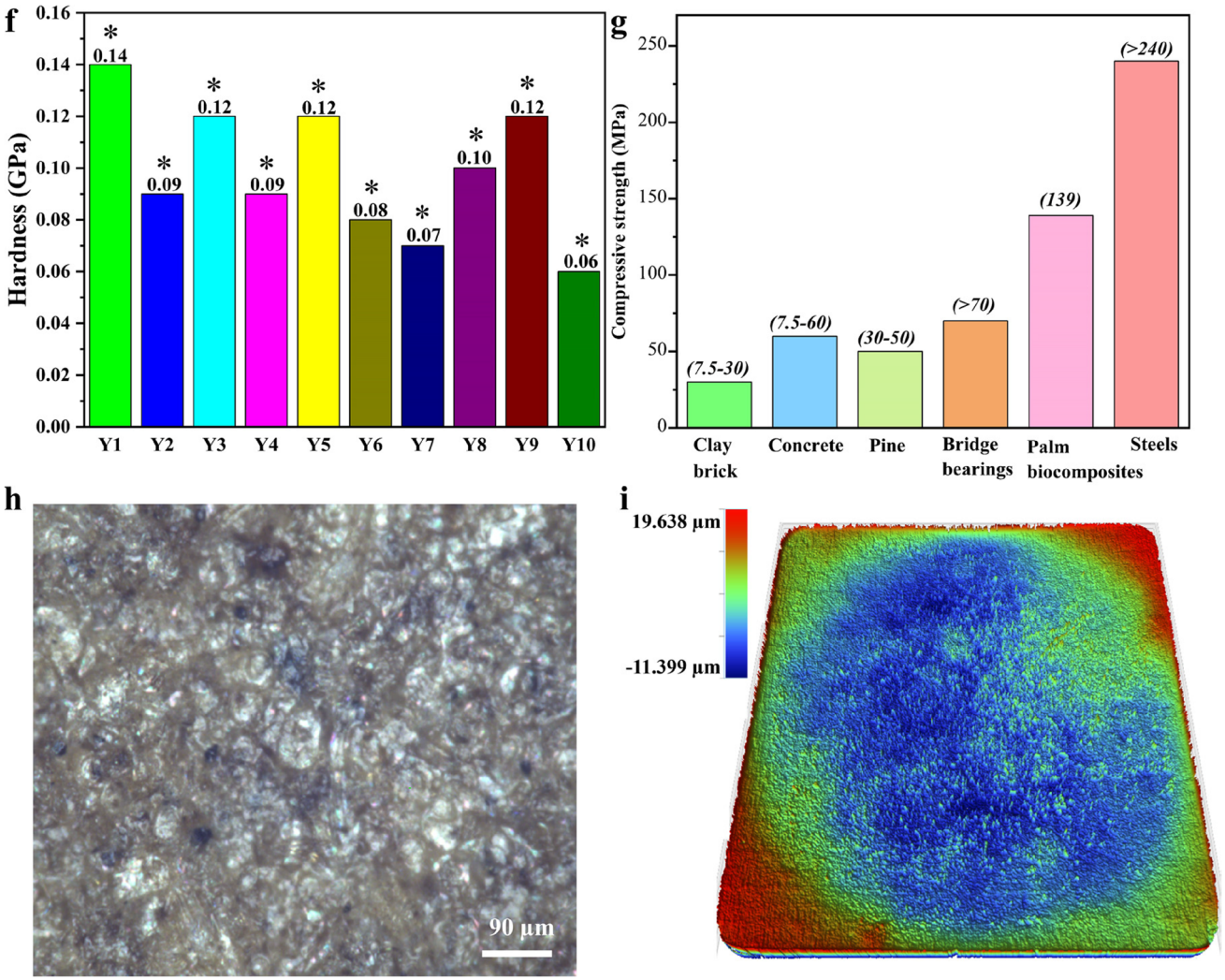

Fig. 3 (continued)

[46, 47]. The test results indicate that as the indentation depth increases, the elastic modulus (Fig. 3e) and hardness (Fig. 3f) of the material also change. From the figure, it can be seen that the Y1 sample has the highest modulus and hardness, reaching 2.16 GPa and 0.14 GPa, the scratch hardness is 7 times that of natural wood (0.02 GPa) [44]. The modulus and hardness of the Y3 sample with high internal adhesive strength are 1.70 GPa and 0.12 GPa, respectively. The Y10 sample with added paraffin has relatively low modulus and hardness, which are 1.30 GPa and 0.06 GPa, respectively. Figure 3h and 3i shows the surface morphology of palm biocomposites after nanoindentation. When heating and cooling palm wood biocomposites, a dense interface layer is formed, forming high adhesive strength, resulting in the interwoven cell walls leading to a high density of natural polymer biocomposites [48]. Therefore, this method enhances both bonding strength and interwoven cell walls, collectively contributing to the method of a high-strength interface layer in natural fiber biocomposites.

3.3 Friction resistance and stability

To further investigate the hardness and internal structure of palm biocomposites, nano scratch tests were conducted on each biocomposite specimen. The study of adhesion between fiber and matrix is often achieved through micromechanical tests. Nano scratch test is an effective means to evaluate Strength of materials properties, and has a wide range of applications in the research of structural material surface [49, 50]. In the experiment, a scratch head with a radius of 0.1 µm was used to test the scratches on the biocomposites under a loading force of 10 N, and a 20×confocal lens was used to image the scratch morphology. Figure 4a and b shows the 3D interface of palm wood under nanoscratching, with each dark color representing different depths. The

maximum scratch depth of each palm biocomposites under the same conditions is shown in Fig. 4d, with Y1 and Y3 having the shallowest maximum scratch depths of 164.9 and 162.0 μm, respectively. Y5 has the maximum scratch depth of 284.9 μm. Under the same force, Y3 has the smallest deformation amplitude and Y5 has the largest change. The maximum scratch depth of Y10 with added paraffin is 183.7 μm.

Plastic resistance (PR) characterizes the ability of a scratched material to resist permanent deformation [51], calculated by dividing the normal force (Fn) by the residual depth (Rd):$PR = \frac{Fn}{Rd}$. Materials with higher PR values have better resistance to permanent scratching. Tests have shown that palm biocomposites Y1 and Y3 have higher PR values and better friction resistance.

In addition to nanoindentation and nanoscratch tests, friction and wear tests to study and compare the surface roughness of palm biocomposites. In the experiment, a grinding ball with a radius of 9.3 mm was used to rub the sample for 10 min under a loading force of 5 N, a frequency of 1 HZ, and a friction condition of 10 mm. The morphology of the friction sample was imaged (Fig. 4c). After 10 min of friction testing under a force of 5 N, the maximum friction depth of Y1 sample is 279.8 μm, Y2 sample is 246.3 μm, Y3 sample is 331.6 μm, while Y7 sample is 48.4 μm, Y8 sample is 56.7 μm, Y9 sample is 24.0 μm, and Y10 sample is 16.6 μm (Fig. 4e). Among them, the Y10 sample has the smallest surface friction depth and the highest smoothness, which also reflects that after adding paraffin, the roughness of the formed biocomposites is reduced, making the surface smoother and more wear-resistant. Secondly, the maximum friction depth of Y7, Y8, and Y9 samples is also within 100 μm, and the wear resistance of the samples is better than other groups.

3.4 Lightweight, compact and environmentally friendly

The samples were scanned and imaged using recon resolutions of 7.5 μm and 22.0 μm, respectively, to obtain virtual slices of the Y1 biocomposites (Fig. 5a and b). From the displayed results, it can be seen the distribution of high-density substances, pores, and wood fibers in the biocomposites. Simultaneously, Dragonfly software was used to directly render the Y1 biocomposites sample to obtain its rendered image (Fig. 5c and d), with different colors representing

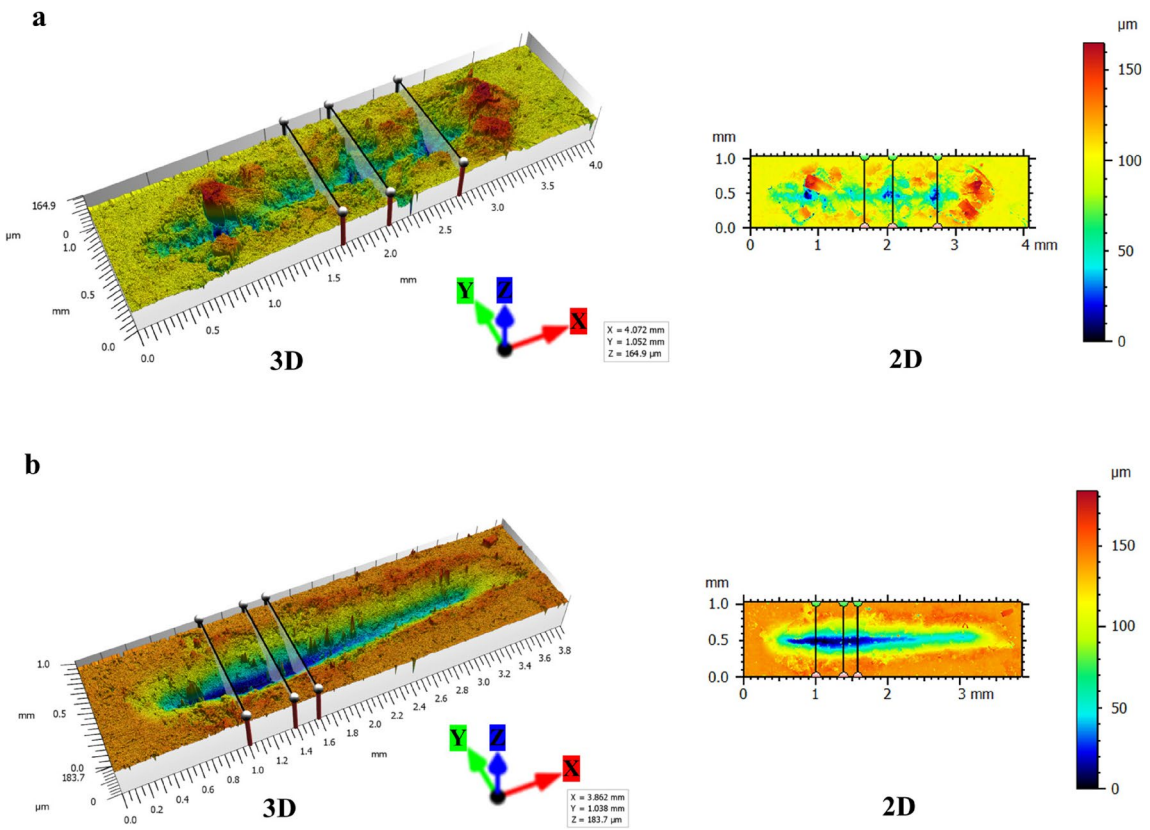

Fig. 4 **a** 3D imaging of palm biocomposites (Y1) by nano-scratch. **b** 3D imaging of palm biocomposites (Y10) by nano-scratch. **c** 3D imaging of palm biocomposites (Y1) by abrasion test. **d** Maximum depth of palm biocomposites by nano-scratch. **e** Maximum depth of palm biocomposites by abrasion test

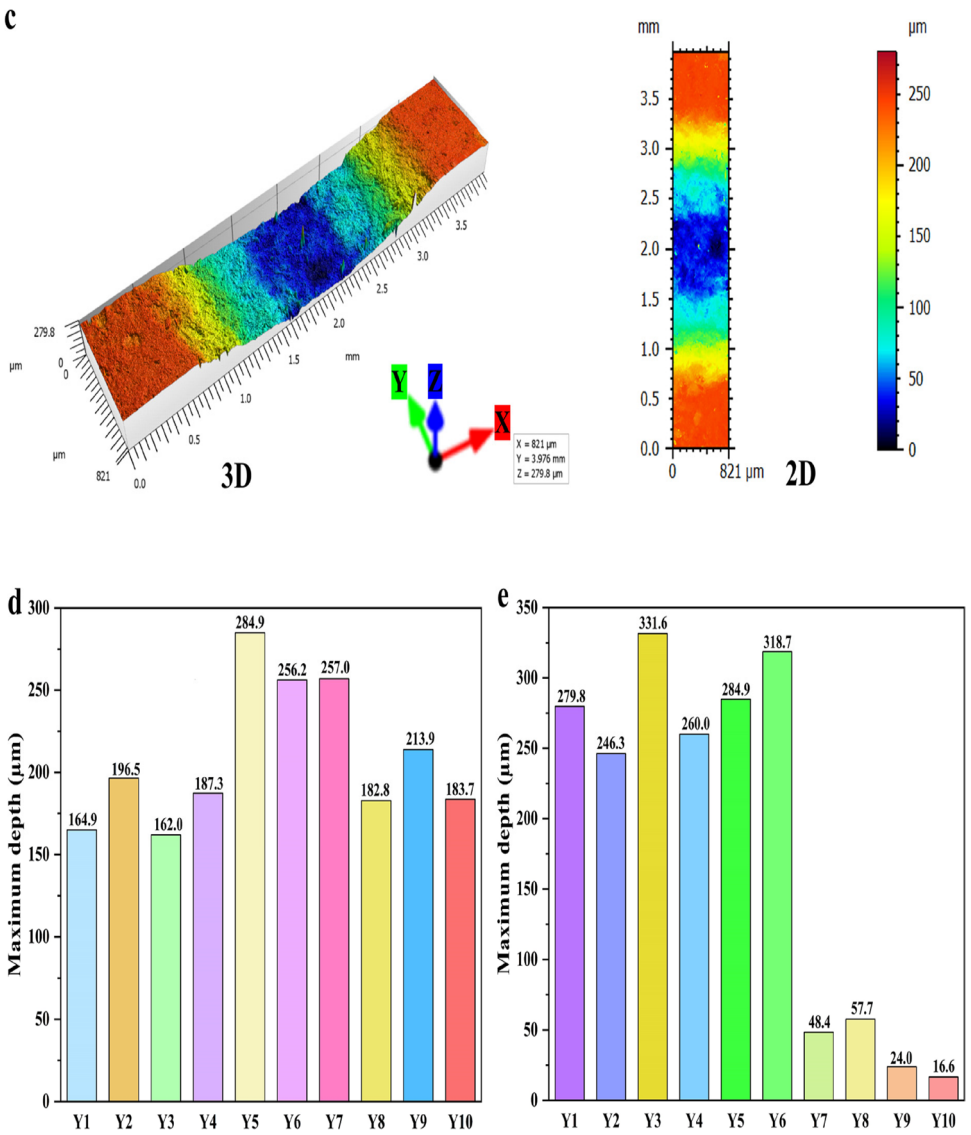

Fig. 4 (continued)

different grayscale values. The morphology of the pores inside the sample plate and their spatial distribution in three-dimensional space are visually displayed. By comparing the volume of pores with that of biocomposites, it was calculated that at a resolution of 22.0 μm recon, the pore volume of Y1 biocomposites in the selected area accounted for 0.67% of the total volume of the selected area. At the same time, under identical conditions, scanning was conducted on Y3 and Y10 biocomposites with high internal bonding strength. According to the results, the porosity of Y1 biocomposites is only 0.67%, while that of Y3 biocomposites is 0.75%. However, due to the addition of paraffin, the porosity of Y10 biocomposites is relatively large, reaching 1.42%. The microscopic CT analysis confirms that the Tight junction fiber network forms a dense interface structure in the palm composite. Figure 5e and f shows the fragmentation of wood cells, which produce various subminiature bonding substances, enhancing the physical and chemical interconnections inside the palm biocomposites, thereby improving its densification.

The formaldehyde release from palm biocomposites was measured, and according to the measurement results (Table S4), the moisture content of the sample is 6.1%, and the formaldehyde release of the Y1-Y10 sample is between 0.9 and 1.3 mg/100 g. Among them, the formaldehyde release of the Y3 sample is the lowest at 0.9 mg/100 g, and the formaldehyde release of the Y10 sample is the highest at 1.3 mg/100 g.

According to the Chinese national standard "Indoor decorating and refurbishing materials Limit of formaldehyde

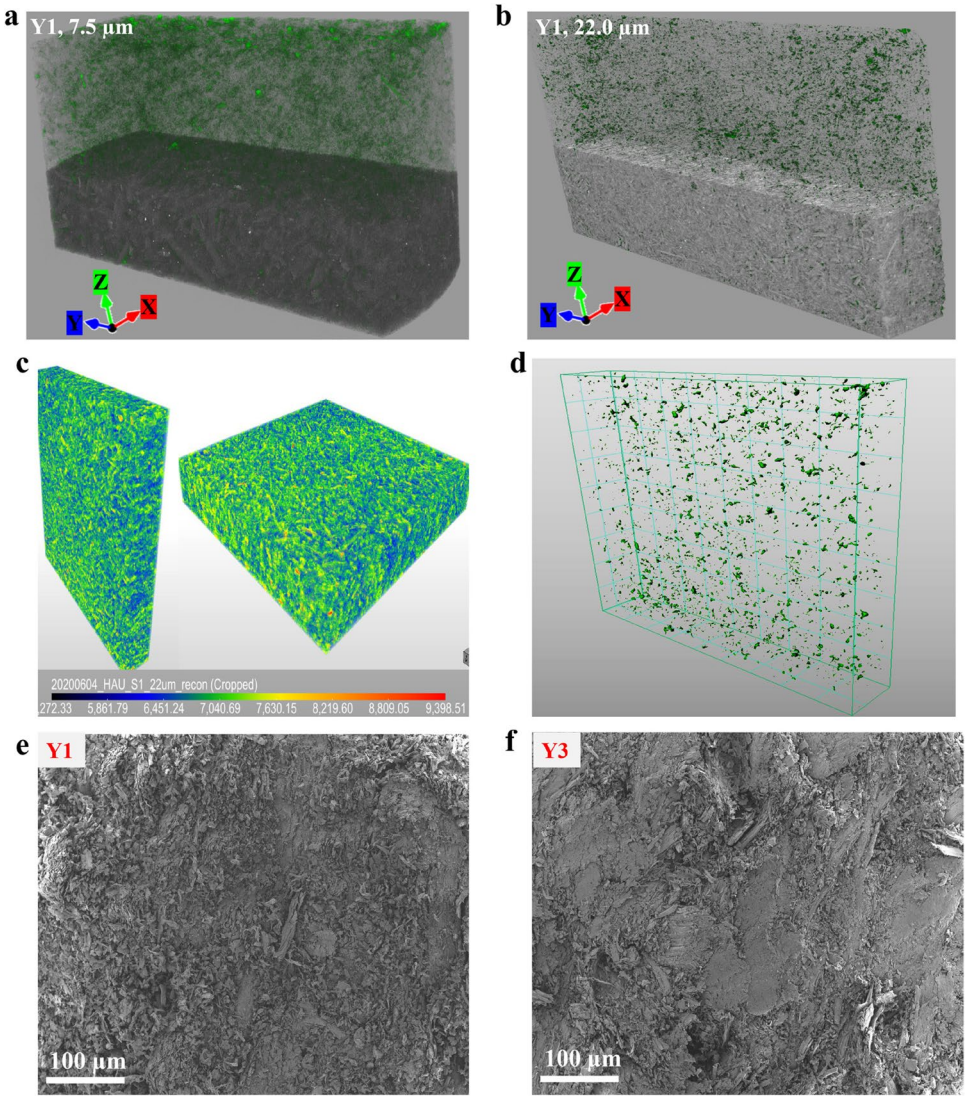

Fig. 5 **a** The recon resolution of palm biocomposites (Y1) scanned by Micro-CT is 7.5 µm. **b** The recon resolution of palm biocomposites (Y1) scanned by Micro-CT is 22.0 µm. **c** 3D rendering of palm biocomposites (Y1) in 22.0 µm recon. **d** Micro-CT photos of biocomposites (Y1) in 22.0 µm recon. **e** SEM micrographs of biocomposites (Y1). **f** SEM micrographs of biocomposites (Y3)

emission of wood based panels and finishing products" (*GB 18580–2001*), the formaldehyde emission of Class A solid wood composite flooring is less than or equal to 9 mg/100 g; the formaldehyde emission of Class B solid wood composite flooring is equivalent to 9–40 mg/100 g [52, 53], and palm biocomposites fully meet the standards for being used as solid wood composite flooring. According to the measurement results of Peng et al. [54] on formaldehyde emission from several kinds of wood, the formaldehyde emission from *Pinus massoniana* is 2.55 mg/100 g, that from *Fraxinus mandshurica* is 3.28 mg/100 g, that from *Cunninghamia lanceolata* is 2.01 mg/100 g, that from *Populus* L. is 1.17 mg/100 g, and that from *Eucalyptus salicifolia* is 1.43 mg/100 g. Compared with the reported results, the formaldehyde emission of palm biocomposites is lower than that of *Pinus massoniana*, *Fraxinus mandshurica*, *Cunninghamia lanceolata*, and *Liueucalyptus*, and close to that of natural *Populus*.

This innovative biocomposites not only represents a groundbreaking technological advancement but also presents sustainability advantages, characterized by low energy consumption and the absence of toxic adhesives. It's a heraldic achievement in the green materials' field that points towards a healthier, more environmentally sound future. The biomaterial's eco-friendliness goes beyond its production process. It also boasts excellent mechanical properties—a key factor for various engineering applications—such as, biocomposites have shown significant improvements in internal bond strength, material density, and resistance to pressure, friction, and environmental influences. This statement highlights an innovative approach utilizing hot pressing, characterized by minimal energy consumption and the absence of adhesives, to transform palm wood biomass into natural and sustainable biocomposites. These biocomposites offer significant potential in the furniture and construction industries, aligning well with contemporary societal preferences

for environmentally friendly materials. This method not only underscores sustainability but also emphasizes the importance of reducing energy consumption and eliminating harmful chemicals, contributing to a greener future. Moreover, by repurposing palm wood biomass, it addresses both environmental concerns and the growing demand for eco-friendly alternatives in various sectors, thus reflecting a promising avenue for sustainable material innovation.

4 Conclusions

An innovative approach has been introduced for the conversion of palm biocomposites into natural and sustainable biocomposites, deemed suitable for application in construction and furniture manufacturing. This method effectively integrates hot pressing with minimal energy consumption, thereby completely eliminating the need for adhesives. The result analyses have shown that the exceptional internal strength of this biocomposites results from a combination of mechanical interlocking and the formation of hydrogen, ether, and ester bonds, which function synergistically like a meticulously assembled puzzle. Compared to conventional materials that rely on formaldehyde-based adhesives, this biocomposites demonstrates enhancements in internal bonding strength—increasing fourfold—while maintaining a low density, which enhances its resilience and environmental friendliness. Additionally, the absence of toxic adhesives not only mitigates concerns about harmful formaldehyde VOCs emissions but also significantly improves indoor air quality. This approach, which combines fragment riveting and cell folding, represents a breakthrough in adhesive-free bonding for wood, achieving original theoretical innovations in formaldehyde-free wood composite materials and offering a novel solution for the development of new structural and furniture materials.

Supplementary Information The online version contains supplementary material available at https://doi.org/10.1007/s42114-024-00940-4.

Acknowledgements All the authors thank associate professor Shengbo Ge for revising the manuscript. The authors acknowledge Henan Agricultural University and for the financial, facility, and technical support throughout this research under a Research Collaboration Agreement (RCA) with Universiti Malaysia Terengganu. The authors also acknowledge Saveetha Institute of Medical and Technical Sciences and Sohar University under a Memorandum of Understanding (MOU) for Research Collaboration with Universiti Malaysia Terengganu. The authors extend their appreciation to the Deanship of Scientific Research at Northern Border University, Arar, KSA for funding this research work through the project number "NBU-FPEJ-2024 -128-03".

Author contribution Yan Yang: Writing—original draft, Visualization, Methodology, Conceptualization. Xiaochen Yue: Writing—original draft, Visualization, Methodology, Conceptualization. Cheng Li: Visualization. Zeinhom M. El-Bahy, Saad Melhi, Hamdy Khamees Thabet: Writing—review & editing. Xiaoyi Duan: Visualization. Nyuk Ling Ma: Writing—review & editing. Yafeng Yang: Writing—review & editing, Supervision, Conceptualization. Su Shiung Lam: Writing—review & editing, Supervision, Conceptualization. Wanxi Peng: Methodology, Writing—review & editing, Supervision, Funding acquisition, Conceptualization.

Funding This work was financially supported by the Longzi Lake New Energy Laboratory project (No. LZHLH2023010) and Zhongyuan Scholar Workstation Funding Project (No.224400520013 and No.234400510016).

Data Availability Statement No datasets were generated or analysed during the current study.

Declarations

Institutional Review Board Statement Not applicable.

Informed Consent Statement Not applicable.

Conflict of interest The authors declare no competing interests.

References

1. Cabeza LF, Boquera L, Chàfer M, Vérez D (2021) Embodied energy and embodied carbon of structural building materials: worldwide progress and barriers through literature map analysis. Energy and Buildings 231:110612. https://doi.org/10.1016/j.enbuild.2020.110612
2. Zhang H, Li S, Hang H, Wang R, Cheng C, Fedorovich KV, Mai X. Mildew-resistant wood building materials with titanium oxide nanosheet. Engineered Science, 2023, 21:816. https://doi.org/10.30919/es8e816
3. Beims RF, Rizkalla A, Kermanshahi-pour A, Xu CC (2023) Reengineering wood into a high-strength, and lightweight bio-composite material for structural applications. Chem Eng J 454:139896. https://doi.org/10.1016/j.cej.2022.139896
4. Li Z, Chen C, Xie H, Yao Y, Zhang X, Brozena A, Li J, Ding Y, Zhao X, Hong M, Qiao H, Smith LM, Pan X, Briber R, Shi SQ, Hu L (2022) Sustainable high-strength macrofibres extracted from natural bamboo. Nature Sustainability 5(3):235–244. https://doi.org/10.1038/s41893-021-00831-2
5. Xiao S, Chen C, Xia Q, Liu Y, Yao Y, Chen Q, Hartsfield M, Brozena A, Tu K, Eichhorn SJ, Yao Y, Li J, Gan W, Shi SQ, Yang VW, Lo Ricco M, Zhu JY, Burgert I, Luo A, Li T, Hu L (2021) Lightweight, strong, moldable wood via cell wall engineering as a sustainable structural material. Science 374(6566):465–471. https://doi.org/10.1126/science.abg9556
6. Dong X, Gan W, Shang Y, Tang J, Wang Y, Cao Z, Xie Y, Liu J, Bai L, Li J, Rojas OJ (2022) Low-value wood for sustainable high-performance structural materials. Nature Sustainability 5(7):628–635. https://doi.org/10.1038/s41893-022-00887-8
7. Zhang H, Wang R, Wang L, Li S, Yuan Y, Wang N, Chen S, Mai X. Super-hydrophobic wood composite with plexiglass coating. Engineered Science, 2023, 23:865. https://doi.org/10.30919/es8d865
8. Ruan J, Chang Z, Rong H, Alomar TS, Zhu D, AlMasoud N, Liao Y, Zhao R, Zhao X, Li Y, Xu BB, Guo Z, El-Bahy ZM, Li H, Zhang X, Ge S (2023) High-conductivity nickel shells encapsulated wood-derived porous carbon for improved electromagnetic interference shielding. Carbon 213:118208. https://doi.org/10.1016/j.carbon.2023.118208
9. Rimdusit S, Kampangsaeree N, Tanthapanichakoon W, Takeichi T, Suppakarn N (2007) Development of wood-substituted

composites from highly filled polybenzoxazine–phenolic novolac alloys. Polym Eng Sci 47(2):140–149. https://doi.org/10.1002/pen.20683
10. Lian M, Huang Y, Liu Y, Jiang D, Wu Z, Li B, Xu Q, Murugadoss V, Jiang Q, Huang M, Guo Z (2022) An overview of regenerable wood-based composites: preparation and applications for flame retardancy, enhanced mechanical properties, biomimicry, and transparency energy saving. Advanced Composites and Hybrid Materials 5(3):1612–1657. https://doi.org/10.1007/s42114-022-00475-6
11. Maddodi BS, Devesh S, Rao A, Shenoy G, Wijerathne H, Sooriyaperkasam N. Repurposing plastic wastes in non-conventional engineered wood building bricks for constructional application-a mechanical characterization using experimental and statistical analysin. Engineered Science, 2022, 18:329–36. https://doi.org/10.30919/es8d696
12. Peng W-X, Yue X, Chen H, Ma NL, Quan Z, Yu Q, Wei Z, Guan R, Lam SS, Rinklebe J, Zhang D, Zhang B, Bolan N, Kirkham MB, Sonne C (2022) A review of plants formaldehyde metabolism: Implications for hazardous emissions and phytoremediation. J Hazard Mater 436:129304. https://doi.org/10.1016/j.jhazmat.2022.129304
13. Lei H, Du G, Pizzi A, Celzard A, Fang Q. Influence of nanoclay on phenol-formaldehyde and phenol-urea-formaldehyde resins for wood adhesives. Journal of Adhesion Science and Technology, 2010, 24: (8–10):1567–76. https://doi.org/10.1163/016942410X500945
14. Khoo SC, Peng WX, Yang Y, Ge SB, Soon CF, Ma NL, Sonne C (2020) Development of formaldehyde-free bio-board produced from mushroom mycelium and substrate waste. J Hazard Mater 400:123296. https://doi.org/10.1016/j.jhazmat.2020.123296
15. Yang Y, Zhang Z, Zhang L, Song F, Ren Y, Zhang X, Zhang J, Liew RK, Foong SY, Chong WWF, Lam SS, Verma M, Ng HS, Sonne C, Ge S (2023) Recent advances in the control of volatile organic compounds emissions from indoor wood-based panels: a comprehensive review. Sci Total Environ 884:163741. https://doi.org/10.1016/j.scitotenv.2023.163741
16. Soni V, Singh P, Shree V, Goel V (2018) Effects of VOCs on human health. In: Sharma N, Agarwal AK, Eastwood P, Gupta T, Singh AP (eds) Air pollution and control. Springer Singapore, Singapore, pp 119–142
17. Yang Y, Kang X, Yang Y, Ye H, Jiang J, Zheng G, Wei K, Ge S, Lam SS, Ouyang H, Chen X, Peng W (2023) Research progress in green preparation of advanced wood-based composites. Advanced Composites and Hybrid Materials 6(6):202. https://doi.org/10.1007/s42114-023-00770-w
18. Yang Y, Zhang L, Zhang J, Ren Y, Huo H, Zhang X, Huang K, Rezakazemi M, Zhang Z (2023) Fabrication of environmentally, high-strength, fire-retardant biocomposites from small-diameter wood lignin in situ reinforced cellulose matrix. Advanced Composites and Hybrid Materials 6(4):140. https://doi.org/10.1007/s42114-023-00721-5
19. Yang Y, Zhang L, Zhang J, Ren Y, Huo H, Zhang X, Huang K, Zhang Z (2023) Reengineering waste boxwood powder into light and high-strength biodegradable composites to replace petroleum-based synthetic materials. ACS Appl Mater Interfaces 15(3):4505–4515. https://doi.org/10.1021/acsami.2c19844
20. George M, Chae M, Bressler DC (2016) Composite materials with bast fibres: structural, technical, and environmental properties. Prog Mater Sci 83:1–23. https://doi.org/10.1016/j.pmatsci.2016.04.002
21. Andrew JJ, Dhakal HN (2022) Sustainable biobased composites for advanced applications: recent trends and future opportunities – a critical review. Composites Part C: Open Access 7:100220. https://doi.org/10.1016/j.jcomc.2021.100220
22. Han Y, Wang Y, Zhao B, Bai Y, Han S, Zhang Y, Li S, Chen Z, Si C, Yu H, Zhang C, Yu W. Carbon dots: building a robust optical shield for wood preservation. Advanced Composites and Hybrid Materials, 2023, 6: (1):39. https://doi.org/10.1007/s42114-022-00619-8
23. Liu X, Liu H, Xu H, Xie W, Li M, Liu J, Liu G, Weidenkaff A, Riedel R (2022) Natural wood templated hierarchically cellular NbC/Pyrolytic carbon foams as stiff, lightweight and high-performance electromagnetic shielding materials. J Colloid Interface Sci 606:1543–1553. https://doi.org/10.1016/j.jcis.2021.08.110
24. Mei H, Huang W, Hua C, Xu Y, Cheng L (2018) A novel approach to strengthen naturally pored wood for highly efficient photodegradation. Carbon 139:378–385. https://doi.org/10.1016/j.carbon.2018.06.073
25. Zemp DC, Guerrero-Ramirez N, Brambach F, Darras K, Grass I, Potapov A, Röll A, Arimond I, Ballauff J, Behling H, Berkelmann D, Biagioni S, Buchori D, Craven D, Daniel R, Gailing O, Ellsäßer F, Fardiansah R, Hennings N, Irawan B, Khokthong W, Krashevska V, Krause A, Kückes J, Li K, Lorenz H, Maraun M, Merk MS, Moura CCM, Mulyani YA, Paterno GB, Pebrianti HD, Polle A, Prameswari DA, Sachsenmaier L, Scheu S, Schneider D, Setiajiati F, Setyaningsih CA, Sundawati L, Tscharntke T, Wollni M, Hölscher D, Kreft H (2023) Tree islands enhance biodiversity and functioning in oil palm landscapes. Nature 618(7964):316–321. https://doi.org/10.1038/s41586-023-06086-5
26. Zhao J, Elmore AJ, Lee JSH, Numata I, Zhang X, Cochrane MA (2023) Replanting and yield increase strategies for alleviating the potential decline in palm oil production in Indonesia. Agric Syst 210:103714. https://doi.org/10.1016/j.agsy.2023.103714
27. Mohd Najib NE, Kanniah KD, Cracknell AP, Yu LJF (2020) Synergy of active and passive remote sensing data for effective mapping of oil palm plantation in Malaysia. Forests 11(8):858. https://doi.org/10.3390/f11080858
28. Escallon-Barrios M, Castillo-Gomez D, Leal J, Montenegro C, Medaglia AL (2022) Improving harvesting operations in an oil palm plantation. Ann Oper Res 314(2):411–449. https://doi.org/10.1007/s10479-020-03686-6
29. Khalil H, Fazita MRN, Bhat AH, Jawaid M, Fuad NAN (2010) Development and material properties of new hybrid plywood from oil palm biomass. Mater Des 31(1):417–424. https://doi.org/10.1016/j.matdes.2009.05.040
30. Mokhtar A, Hassan K, Aziz AA, Wahid MB (2011) Plywood from oil palm trunks. Journal of Oil Palm Research 23:1159–1165
31. Ge S, Ma NL, Jiang S, Ok YS, Lam SS, Li C, Shi SQ, Nie X, Qiu Y, Li D, Wu Q, Tsang DCW, Peng W, Sonne C (2020) Processed bamboo as a novel formaldehyde-free high-performance furniture biocomposite. ACS Appl Mater Interfaces 12(27):30824–30832. https://doi.org/10.1021/acsami.0c07448
32. Chauhan M, Gupta M, Singh B, Singh AK, Gupta VK (2012) Pine needle/isocyanate composites: dimensional stability, biological resistance, flammability, and thermoacoustic characteristics. Polym Compos 33(3):324–335. https://doi.org/10.1002/pc.22151
33. Lee H, Jeong S, Cho S, Chung W (2020) Enhanced bonding behavior of multi-walled carbon nanotube cement composites and reinforcing bars. Compos Struct 243:112201. https://doi.org/10.1016/j.compstruct.2020.112201
34. Hardiman M, Vaughan TJ, McCarthy T (2017) A review of key developments and pertinent issues in nanoindentation testing of fibre reinforced plastic microstructures. Compos Struct 180:782–798. https://doi.org/10.1016/j.compstruct.2017.08.004
35. Wang X, Xu P, Han R, Ren J, Li L, Han N, Xing F, Zhu J (2019) A review on the mechanical properties for thin film and block structure characterised by using nanoscratch test. Nanotechnol Rev 8(1):628–644. https://doi.org/10.1515/ntrev-2019-0055
36. Wei XF, Li WJ, Liang BJ, Li BL, Zhang JJ, Zhang LS, Wang ZB (2016) Surface modification of Co-Cr-Mo implant alloy by laser interference lithography. Tribol Int 97:212–217. https://doi.org/10.1016/j.triboint.2016.01.039

37. Cao JL, Teng H, Wang WR, Wei XC, Zhao HS (2022) Tribological properties of the 40Cr/GCr15 tribo-pair under unidirectional rotary and reciprocating dry sliding. Coatings 12(5):557. https://doi.org/10.3390/coatings12050557
38. Wentzel M, Rolleri A, Pesenti H, Militz H (2019) Chemical analysis and cellulose crystallinity of thermally modified Eucalyptus nitens wood from open and closed reactor systems using FTIR and X-ray crystallography. European Journal of Wood and Wood Products 77(4):517–525. https://doi.org/10.1007/s00107-019-01411-0
39. Hao YN, Pan YF, Du R, Wang YM, Chen ZJ, Zhang XT, Wang XM (2018) The influence of a thermal treatment on the decay resistance of wood via FTIR analysis. Adv Mater Sci Eng 2018:8461407. https://doi.org/10.1155/2018/8461407
40. Colom X, Carrillo F, Nogues F, Garriga P (2003) Structural analysis of photodegraded wood by means of FTIR spectroscopy. Polym Degrad Stab 80(3):543–549. https://doi.org/10.1016/S0141-3910(03)00051-X
41. Zhu XD, Xue YY, Zhang SJ, Zhang J, Shen J, Yi SL, Gao Y. Mechanics and crystallinity/thermogravimetric investigation into the influence of the welding time and CuCl2 on wood dowel welding. BioResources, 2018, 13(1):1329–47. https://doi.org/10.15376/biores.13.1.1329-1347
42. Tourani H, Molazemhosseini A, Khavandi A, Mirdamadi S, Shokrgozar MA, Mehrjoo M (2013) Effects of fibers and nanoparticles reinforcements on the mechanical and biological properties of hybrid composite polyetheretherketone/short carbon fiber/nano-SiO2. Polym Compos 34(11):1961–1969. https://doi.org/10.1002/pc.22603
43. Shi Y, Jiang J, Ye H, Sheng Y, Zhou Y, Foong SY, Sonne C, Chong WWF, Lam SS, Xie Y, Li J, Ge S (2023) Transforming municipal cotton waste into a multilayer fibre biocomposite with high strength. Environ Res 218:114967. https://doi.org/10.1016/j.envres.2022.114967
44. Song J, Chen C, Zhu S, Zhu M, Dai J, Ray U, Li Y, Kuang Y, Li Y, Quispe N, Yao Y, Gong A, Leiste UH, Bruck HA, Zhu JY, Vellore A, Li H, Minus ML, Jia Z, Martini A, Li T, Hu L (2018) Processing bulk natural wood into a high-performance structural material. Nature 554(7691):224–228. https://doi.org/10.1038/nature25476
45. Li H, Alam MS (2024) Exploring key factors affecting the ultimate compression capacity of unbonded steel-mesh-reinforced Rubber Bearings. Eng Struct 306:117813. https://doi.org/10.1016/j.engstruct.2024.117813
46. Bourmaud A, Baley C (2010) Effects of thermo mechanical processing on the mechanical properties of biocomposite flax fibers evaluated by nanoindentation. Polym Degrad Stab 95(9):1488–1494. https://doi.org/10.1016/j.polymdegradstab.2010.06.022
47. Sahari J, Sapuan SM, Zainudin ES, Ishak MR, Maleque MA, Zuhri MYM, Akhtar R (2017) Nanoindentation and the low velocity impact response of biofibre, biopolymer and its biocomposite derived from sugar palm tree. Curr Org Synth 14(2):227–232. https://doi.org/10.2174/1570179413666160831122841
48. Chen X, Ashcroft IA, Wildman RD, Tuck CJ (2027) A combined inverse finite element - elastoplastic modelling method to simulate the size-effect in nanoindentation and characterise materials from the nano to micro-scale. Int J Solids Struct 104:25–34. https://doi.org/10.1016/j.ijsolstr.2016.11.004
49. Chen J, An QL, Chen M (2020) Transformation of fracture mechanism and damage behavior of ceramic-matrix composites during nano-scratching. Composites Part A-Applied Science and Manufacturing 130:105756. https://doi.org/10.1016/j.compositesa.2019.105756
50. Liu JH, Zeng Q, Xu SL (2020) The state-of-art in characterizing the micro/nano-structure and mechanical properties of cement-based materials via scratch test. Constr Build Mater 254:119255. https://doi.org/10.1016/j.conbuildmat.2020.119255
51. Pugno NM, Calabri L (2012) Nanoindentation and nanoscratch of hybrid metallic-organic framework material. Mater Sci Technol 28(9–10):1156–1160. https://doi.org/10.1179/1743284712Y.0000000001
52. Song W, Cao Y, Wang DD, Hou GJ, Shen ZH, Zhang SB (2015) An investigation on formaldehyde emission characteristics of wood building materials in Chinese Standard Tests: product emission levels, measurement uncertainties, and data correlations between various tests. PLoS ONE 10(12):e0144374. https://doi.org/10.1371/journal.pone.0144374
53. Kim S, Kim JA, Kim HJ, Lee HH, Yoon DW (2006) The effects of edge sealing treatment applied to wood-based composites on formaldehyde emission by desiccator test method. Polym Testing 25(7):904–911. https://doi.org/10.1016/j.polymertesting.2006.05.010
54. Peng WX, Yue XC, Chen HL, Ma NL, Quan Z, Yu Q, Wei ZH, Guan RR, Lam SS, Rinklebe J, Zhang DQ, Zhang BH, Bolan N, Kirkham MB, Sonne C (2022) A review of plants formaldehyde metabolism: implications for hazardous emissions and phytoremediation. Journal of Hazardous Materials 436:129304. https://doi.org/10.1016/j.jhazmat.2022.129304

Authors and Affiliations

Yan Yang[1,2] · Xiaochen Yue[1] · Cheng Li[1] · Zeinhom M. El-Bahy[3] · Saad Melhi[4] · Hamdy Khamees Thabet[5] · Xiaoyi Duan[1] · Nyuk Ling Ma[6,7] · Yafeng Yang[1] · Su Shiung Lam[2,8] · Wanxi Peng[1]

✉ Wanxi Peng
pengwanxi@163.com

[1] School of Forestry, School of Landscape Architecture and Art, Henan Agricultural University, Zhengzhou 450002, China

[2] Higher Institution Centre of Excellence (HICoE), Institute of Tropical Aquaculture and Fisheries (AKUATROP), Universiti Malaysia Terengganu, Terengganu, Kuala Nerus 21030, Malaysia

[3] Department of Chemistry, Faculty of Science, Al-Azhar University, Nasr City, Cairo 11884, Egypt

[4] Department of Chemistry, College of Science, University of Bisha, Bisha 61922, Saudi Arabia

[5] Department of Chemistry, College of Sciences and Arts, Northern Border University, Rafha 91911, Saudi Arabia

[6] BIOSES Research Interest Group, Faculty of Science & Marine Environment, Universiti Malaysia Terengganu, Terengganu, Kuala Nerus 21030, Malaysia

[7] Center for Global Health Research (CGHR), Saveetha Medical College, Saveetha Institute of Medical and Technical Sciences (SIMATS), Saveetha University, Chennai, India

[8] Faculty of Engineering, Sohar University, PC:311, PO Box 44, Sohar, Oman